

# Wireless Channel Foundation Model with Embedded Noise-Plus-Interference Suppression Structure

Yuwei Wang, Li Sun, Tingting Yang

**Abstract**—Wireless channel foundation model (WCFM) is a task-agnostic AI model that is pretrained on large-scale wireless channel datasets to learn a universal channel feature representation that can be used for a wide range of downstream tasks related to communications and sensing. While existing works on WCFM have demonstrated its great potentials in various tasks including beam prediction, channel prediction, localization, etc, the models are all trained using perfect (i.e., error-free and complete) channel information state (CSI) data which are generated with simulation tools. However, in practical systems where the WCFM is deployed, perfect CSI is not available. Instead, channel estimation needs to be first performed based on pilot signals over a subset of the resource elements (REs) to acquire a noisy version of the CSI (termed as degraded CSI), which significantly differs from the perfect CSI in some real-world environments with severe noise and interference. As a result, the feature representation generated by the WCFM is unable to reflect the characteristics of the true channel, yielding performance degradation in downstream tasks. To address this issue, in this paper we propose an enhanced wireless channel foundation model architecture with noise-plus-interference (NPI) suppression capability. In our approach, coarse estimates of the CSIs are first obtained. With these information, two projection matrices are computed to extract the NPI terms in the received signals, which are further processed by a NPI estimation and subtraction module. Finally, the resultant signal is passed through a CSI completion network to get a clean version of the CSI, which is used for feature extraction. Simulation results demonstrated that compared to the state-of-the-art solutions, WCFM with NPI suppression structure achieves improved performance on channel prediction task.

**Index Terms**—Wireless foundation model, noise-plus-interference suppression structure, channel representations, channel prediction.

## I. INTRODUCTION

Future 6G network is featured by the the integration of communications, sensing, and AI. Compared to 2G~5G networks which are connectivity-oriented, 6G is expected to provide diversified services (communications, localization, environment reconstruction, edge inference, etc.) across a wide range of scenarios. Moreover, stringent requirements are imposed in terms of the reliability, delay, throughput, and so on.

The fulfillment of the aforementioned 6G visions relies heavily on the availability of accurate knowledge of the underlying wireless channels. However, acquiring channel state information (CSI) may incur extremely high overhead

of pilot signalling in future 6G because of the proliferation of antennas, the use of wider frequency bands, and the high mobility of UE. Therefore, obtaining an accurate and universal channel representation with limited pilot overhead emerges as a fundamental and critical challenge in the physical layer design of 6G. Based on existing studies, three typical categories of potential approaches can be identified as possible directions toward addressing this challenge.

The first type includes the traditional model-based CSI measurement methods. To be specific, dedicated pilot signals are utilized to first estimate the CSIs over some specific resource elements (REs), and then channel interpolation or extrapolation techniques are applied to infer the CSIs of other REs or future instants. While this approach has been widely adopted in current cellular systems, it relies on accurate a priori assumptions of channel model (e.g., the spatio-temporal-frequency correlation, the noise distribution, and the stationarity), making it inherently sensitive to model mismatches. Because of the emergence of frequency bands, scenarios, and hardware, it is extremely difficult, if not impossible, to establish an accurate and universal channel model, thereby degrading the performance of model-based method significantly.

The second class of approaches are based on deep learning. In this paradigm, the known pilot signals together with their corresponding received signals are fed into a neural network to extract the channel features in a data driven manner. This method uses deep neural networks to learn the inherent characteristics of wireless channels, without relying on prior knowledge of channel model, and has demonstrated superior performance in terms of channel estimation and prediction accuracy compared to traditional alternatives [1]- [3]. Nevertheless, the adopted AI models and its extracted channel representations are typically task-specific and scenario-specific, which have limited abilities in generalizing to new tasks or unseen scenarios.

Inspired by the emergence of large language model (LLMs) techniques, the approaches of the third type aim at building foundation models for wireless channel representation to empower multiple physical layer tasks. The foundation models are pre-trained on large-scale wireless channel datasets in a task-agnostic and label-free manner, which imparts them strong generalization abilities across various tasks and scenarios. In [4], a LLM-based framework is developed for beam prediction. In this work, the wireless data sequence is reprogrammed into a natural language representation and aligned

The authors are with Department of Network Intelligence, Pengcheng Laboratory, Shenzhen, China (e-mail: wangyw03@pcl.ac.cn; sunl03@pcl.ac.cn; yangtt@pcl.ac.cn).

with the pre-training input format of LLMs, thereby activating the ability of the LLMs to process the wireless time series data. In [5], the multi-modal large model DeepSeek is fine-tuned for beam prediction. In particular, positions of the scatters and multi-view images are first fine-tuned with low-rank adaptation (LoRA) to extract environmental embeddings, and then these embeddings are further processed by the large model to output the optimal beam index. Both of the aforementioned works [4]-[5] rely on the available open-source large language models or multi-modal large models, and utilize fine-tuning techniques to adapt the general-purpose large models to downstream tasks in wireless domain. In contrast with this paradigm, [6]- [8] developed wireless native foundation models and performed training from scratch. In [6], a unified framework of wireless foundation model is developed, which integrates cross-domain embedding, positional encoding, and Transformer encoding to generate universal representations of wireless channels. In [7], a masked auto-encoder (MAE) based network structure is devised for time-frequency channel prediction tasks, and extensive CSI datasets are used for pre-training such that the model can be generalized to various CSI configurations without any fine-tuning. In [8], a task-agnostic model called Large Wireless Model (LWM) was developed to generate universal channel embeddings that can be used across a wide range of downstream tasks such as LoS/NLoS classification, beam prediction, etc.

While the LLM-based methods have demonstrated extraordinary performance in physical layer communications tasks, all of the existing works used perfect CSIs as the input data to train the model. However, in practical wireless systems where the model is deployed, it is impossible to acquire the perfect CSIs. Instead, channel estimation and completion need to be conducted to obtain the estimated CSI from the known pilots and its associated received counterparts. Note that practical wireless systems typically operate in open environments where the signal transmissions are subject to unknown interference and noises, which yields inevitable errors in channel estimation. Based on these erroneous CSIs as inputs, the large AI model will output “biased” feature representations which do not match the realistic channel status. Consequently, the performance of downstream tasks which are realised based upon these feature representations will be significantly degraded.

To deal with the aforementioned challenges, we propose a wireless channel foundation model (WCFM) architecture with embedded noise-plus-interference (NPI) suppression capability. In our proposed design, coarse channel estimates are first obtained using classical algorithms such as least squares (LS), and then two projection modules are applied to extract the NPI components within the channel subspace and its orthogonal subspace, respectively. After that, an NPI estimation network is used to estimate the NPI, which will be further subtracted from the received signals. Finally, a channel refinement and completion network is utilized to form a cleaner version of the channel estimate, which is fed into a feature extractor to obtain the channel representation. The NPI suppression module can be either independently trained or jointly trained with the backbone feature extractor. In either case, the output channel representations are able to reflect the characteristics of wireless

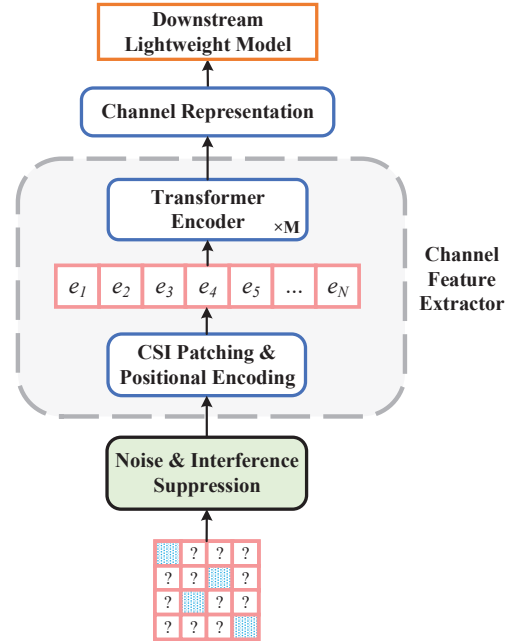


Fig. 1: Wireless foundation model with noise-plus-interference suppression structure.

channels more accurately. As will be shown via simulations, wireless channel foundation model with the proposed NPI suppression structure achieves improved performance over channel prediction task.

## II. NOISE-PLUS-INTERFERENCE SUPPRESSION MODULE

### A. Neural Network Structure

As is shown in Fig. 1, we consider a WCFM which adopts a transformer architecture with multi-head attention mechanisms. The WCFM constitutes of a NPI suppression module, a CSI patching and positional encoding module, and several transformer encoder blocks. The NPI suppression module is used to obtain a clean version of the estimated CSIs from  $\{\mathbf{x}_p, \mathbf{y}_p\}$  pairs, where  $\mathbf{x}_p$  and  $\mathbf{y}_p$  are known pilots and their corresponding received signals, respectively. The transmission of  $\mathbf{x}_p$  may be subject to severe interference and channel noises, yielding the received signal  $\mathbf{y}_p$  to be highly distorted. The CSI patching and positional encoding module encodes the (cleaned) CSI samples into embeddings which are further processed by transformer encoder blocks. The transformer encoder blocks capture the intrinsic relationships and contextual patterns within the data, and outputs a universal channel representation that is suitable for various downstream tasks. Except the NPI suppression module, other modules are almost the same as those adopted by the existing WCFMs in the literature (such as [8]). Therefore, we only introduce the details of the NPI suppression module in the following discussions.

The structure of the NPI suppression module is depicted in Fig. 2. To facilitate the exposition, we consider a MIMO-OFDM communications system with  $N$  transmit antennas and  $M$  receive antennas. Each slot consists of  $L$  OFDM symbols with each containing  $K$  subcarriers. Thus, the wireless channel over any given symbol duration and subcarrier is a  $M \times N$

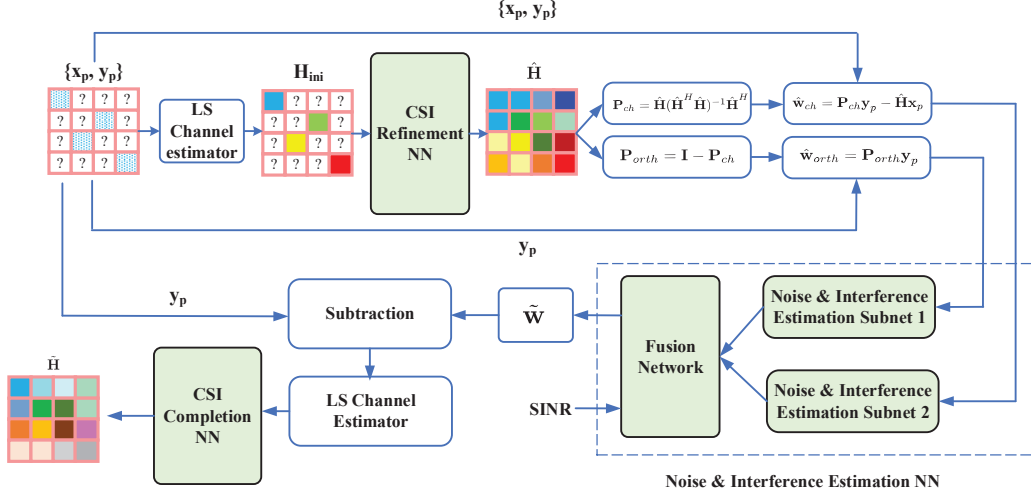


Fig. 2: Noise-Plus-Interference Suppression Structure.

matrix  $\mathbf{H}$  where the entity  $h_{ij}$  is the channel coefficient from transmitter antenna  $j$  to receive antenna  $i$ . Among the  $L \times K$  REs over each slot, it is assumed that  $K_p$  REs (termed as pilot REs hereafter) are occupied by pilots and are used for estimating channels, and the remaining REs (referred to as information REs hereafter) are used for delivering the payloads.

Based on known pilots and the associated received counterparts, the LS algorithm is first applied to form an initial estimate of the CSIs over the pilot REs, denoted by  $H_{ini}$ . Afterwards, a CSI refinement network is built to generate the CSIs across all REs. With supervised training, the CSI refinement network is able to offer an implicit NPI mitigation capability, thus favoring succeeding processing. For ease of exposition, we denote the refined CSIs over pilot REs as  $\hat{\mathbf{H}}$ , which will be used for further NPI suppression.

Once  $\hat{\mathbf{H}}$  is obtained, we are able to derive two projection matrices  $\mathbf{P}_{ch}$  and  $\mathbf{P}_{orth}$ , which are expressed as

$$\mathbf{P}_{ch} = \hat{\mathbf{H}}(\hat{\mathbf{H}}^H \hat{\mathbf{H}})^{-1} \hat{\mathbf{H}}^H, \quad (1)$$

and

$$\mathbf{P}_{orth} = \mathbf{I} - \hat{\mathbf{H}}(\hat{\mathbf{H}}^H \hat{\mathbf{H}})^{-1} \hat{\mathbf{H}}^H, \quad (2)$$

respectively. In (1) and (2),  $\mathbf{I}$  is the identity matrix, and  $(\cdot)^H$  stands for the Hermitian transpose.  $\mathbf{P}_{ch}$  is the projection matrix onto the channel subspace, and  $\mathbf{P}_{orth}$  is the projection matrix onto the subspace that is orthogonal to the channel subspace. By multiplying  $\mathbf{y}_p$  with  $\mathbf{P}_{ch}$  and subtracting  $\hat{\mathbf{H}}\mathbf{x}_p$  from the multiplication, we have

$$\hat{\mathbf{w}}_{ch} = \mathbf{P}_{ch}\mathbf{y}_p - \hat{\mathbf{H}}\mathbf{x}_p, \quad (3)$$

which represents the estimated NPI component in the channel subspace. Similarly, multiplying  $\mathbf{y}_p$  with  $\mathbf{P}_{orth}$  yields the estimated NPI component in the subspace that is orthogonal to the channel subspace, given by

$$\hat{\mathbf{w}}_{orth} = \mathbf{P}_{orth}\mathbf{y}_p. \quad (4)$$

Due to channel estimation errors,  $\hat{\mathbf{w}}_{ch}$  and  $\hat{\mathbf{w}}_{orth}$  contains not only NPI terms, but also residual signal terms. In order to

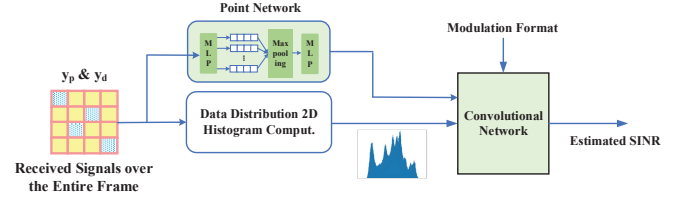


Fig. 3: SINR Estimator.

recover the NPI more accurately, a NPI estimation network is introduced, as is shown in the part outlined by the dashed box.

As illustrated in Fig. 2,  $\hat{\mathbf{w}}_{ch}$  and  $\hat{\mathbf{w}}_{orth}$  are passed through two independent NPI estimation sub-networks, whose outputs are then concatenated and fed into a fusion network to form a final estimate of the entire NPI, denoted by  $\tilde{\mathbf{w}}$ . In addition to the concatenated vector, the fusion network also accepts the system SINR as its input. In this manner, the fusion network combines the two NPI terms  $\hat{\mathbf{w}}_{ch}$  and  $\hat{\mathbf{w}}_{orth}$  flexibly based on varying SINR conditions. In practice, the SINR value is obtained using an SINR estimator, which will be elaborated on later.

Afterwards,  $\tilde{\mathbf{w}}$  is subtracted from  $\mathbf{y}_p$ , resulting in a cleaner version of the received signal  $\tilde{\mathbf{y}}_p$ . Based on  $\tilde{\mathbf{y}}_p$ , an LS channel estimator followed by a completion network is employed to output the refined channel estimates  $\hat{\mathbf{H}}$  over all the REs.  $\hat{\mathbf{H}}$  will be further processed by the channel feature extractor.

Now attention is shifted to the SINR estimator in Fig. 2. This module is used to estimate the average SINR over each slot. The estimated SINR allows the NPI estimation network to learn the ‘‘distortion level’’ of the environment, thereby facilitating the NPI estimation. The structure of the SINR estimator is depicted in Fig. 3, where the received signal symbols of each slot and the associated modulation formats for all these symbols are used as inputs. Note that in practical communications systems, modulation formats are typically known by both the transmitter and the receiver side. The input data is first processed by two modules separately: a 2D histogram generation module and a Point Network.

The 2D histogram generation module computes a 2D histogram which shows the statistical distribution of the received

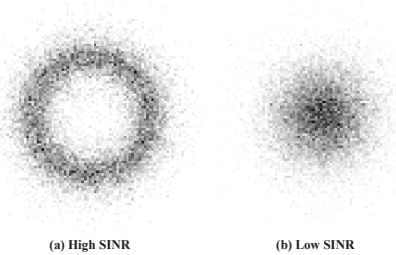


Fig. 4: 2D histogram comparison for high SINR and low SINR cases.

I/Q samples within an OFDM slot on the 2D plane. As is shown in Fig. 4 with QPSK modulation, the histogram pattern varies significantly with SINR. Under high SINR, the distribution of the received signals is mainly shaped by the channel coefficients across subcarriers, time instances, and receive antennas, forming a clear constellation structure. In contrast, under low SINR, noise and interference dominate, causing the received samples to collapse into a single cluster and blur the constellation. In this sense, the 2D histogram characterizes the amplitude range of received signals, thus reflecting how severe the noise-plus-interference is. The Point Network (PointNet) which is widely used to handle the point cloud data, is employed here to capture the “details” of the received data. The received signal sample sequence over each RE is first transformed into a  $d$ -dimensional vector through an MLP layer. Assuming the total number of REs to be  $N_{RE}$ , we have a  $N_{RE} \times d$  matrix after the MLP. Then, a column-wise max-pooling operation is performed to produce a “fluctuation vector”. If the SINR is high (i.e., the impact of noise and interference is negligible), the fluctuation vector will exhibit a small variation pattern. On the other hand, if the SINR is low (i.e., the level of interfering terms is high), the elements within the fluctuation vector will vary over a wide range, due to the random noise and interference. These features will be further extracted through a MLP layer to produce the output of the PointNet. Based on the analysis above, this output also reflects the severeness of the noise-plus-interference. So, by combining the outputs of the PointNet and the 2D-histogram and passing them through a convolutional network, the SINR value can be estimated.

### B. Training Approach

In the NPI suppression model, the CSI refinement network, the NPI estimation network, the CSI completion network, and the SINR estimator are trainable modules, while other parts are non-AI signal processing operations and are thus non-trainable.

The CSI refinement network and the SINR estimator are trained using standard supervised methods with the normalized mean square error (NMSE) as the loss function. With respect to the NPI estimation network and the CSI completion network, we adopt a two-step training paradigm. In the first step, the NPI estimation network is trained using labeled NPI, following a supervised training method to minimize the NMSE. Having trained the NPI estimation network for several rounds, this module will be jointly trained with the

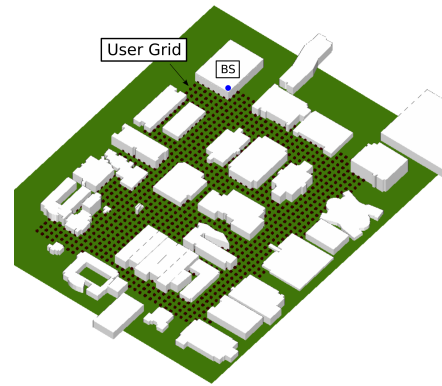


Fig. 5: The ASU Campus scenario.

CSI completion network to minimize the CSI reconstruction error over all the REs. The loss function is:

$$\mathcal{L}_{recon} = NMSE(\tilde{\mathbf{H}}, \mathbf{H}), \quad (5)$$

with  $\mathbf{H}$  being the CSI label.

## III. SIMULATION RESULTS AND DISCUSSIONS

### A. Simulation Setups

In this section, the open source wireless channel generator DeepMIMO [9] is utilized to produce the CSI dataset for both training and evaluation. We use the data collected from the *ASU Campus* scenario to train and evaluate the model. The BS with 32 antennas is deployed at a fixed location, and 80000 single-antenna UEs are distributed randomly within a area, of which 60000 BS-UE CSI samples are used for WCFM training,  $R_t \cdot 20000$  for downstream lightweight model training, and  $(1 - R_t) \cdot 20000$  for testing. Fig. 5 displays an example where “BS” is the base station, and the UEs are distributed in the area of “User Grid”. Each transmission slot consists of 14 OFDM symbols and every symbol spans across 32 subcarriers. The 3rd and 10th OFDM symbols are used for pilot transmission, where the pilots are inserted with a spacing of 6 subcarriers. Other REs within each slot are occupied by payload data.

Based on the received signals at the BS, numerous  $\{\mathbf{x}_p, \mathbf{y}_p\}$  pairs are collected. During the training phase, these pairs with the known CSI and noise-plus-interference label are used to train the network. During the inference phase, Only the  $\{\mathbf{x}_p, \mathbf{y}_p\}$  pairs on the pilot REs and the received payload data  $\{\mathbf{y}_d\}$ ’s are available at the BS, which are fed into the NPI suppression module and the succeeding channel feature extractor to extract channel representations. To specifically evaluate the contribution of the proposed NPI suppression module, the channel feature extractor is not trained in our experiments. Instead, we use the NN parameters from the pre-trained LWM [8] directly. This ensures that the performance gain comes from the NPI suppression module rather than retraining effects.

### B. Downstream Task and Benchmark Schemes

We consider a channel prediction task, which aims to predict CSIs over  $N_p$  adjacent subcarriers based on the existing CSI

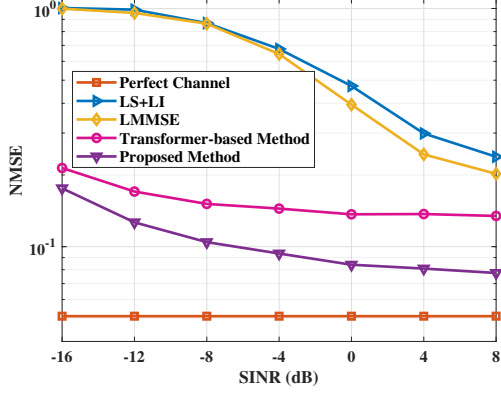


Fig. 6: NMSE versus SINR (dB).

over 32 subcarriers. For comparison, four competing solutions are chosen as benchmarks.

1) LS plus linear interpolation (LS+LI): In this approach, a LS channel estimator is first applied to estimate the CSI over the REs that carry on pilots, and then a linear interpolation algorithm is utilized to obtain the full CSIs across all REs.

2) LMMSE: A LMMSE estimator is used to recover the CSIs of all the REs. This is a widely adopted approach in 5G BS and UE. Note that the channel covariance matrix is required to be available for this method. In our simulations, an exponential function is adopted to model the time–frequency correlation, from which the channel covariance matrix is derived.

3) Transformer-based method: In this method, the LS algorithm is first used for channel estimation to obtain the CSIs over pilot REs, and then a Transformer-based network is deployed to recover the full CSI of all REs.

4) Perfect-CSI: This corresponds to an ideal case where the CSIs over the pilot REs are perfectly known. This case will be used to demonstrate the upper bound of the performance.

For all of the aforementioned benchmarks and our proposed scheme, the inputs are the same, i.e., the  $\{\mathbf{x}_p, \mathbf{y}_p\}$  pairs on the pilot REs and the received payload data  $\{\mathbf{y}_d\}$ 's, and the outputs are the recovered CSIs over all the REs with each slot. These outputs will be fed to the channel feature extractor to output a universal representation of CSIs, which is further processed by a lightweight ResNet [10] model to obtain the final channel prediction results. The channel prediction model is trained with  $R_t \cdot 20000$  CSI representations and evaluated with  $(1 - R_t) \cdot 20000$  CSI representations.

### C. Simulation Results

The downstream task performance in channel prediction, comparing the proposed method with various benchmarks, is presented in Fig. 6, where the number of sub-carriers to be predicted  $N_p$  is 16, and the percentage of downstream training samples  $R_t$  is 50%. As expected, the NMSE of all candidates decreases with the increase in SINR. This is because higher SINR leads to more accurate channel estimation, which in turn yields more precise channel representations and thereby improves the performance of the downstream channel prediction. However, the traditional model-based methods (i.e.,

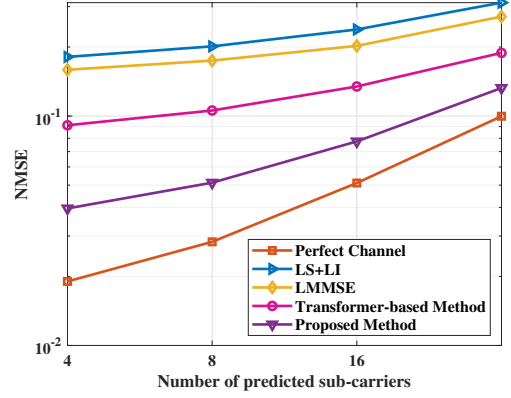


Fig. 7: NMSE versus number of predicted sub-carriers ( $N_p$ ).

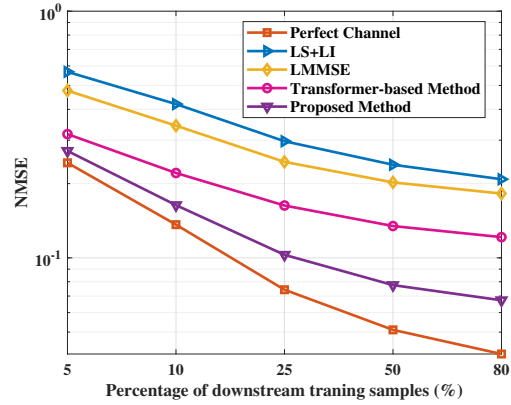


Fig. 8: NMSE versus percentage of downstream training samples ( $R_t$ ).

LS+LI, LMMSE) behave poorly across entire SINR range, since the preset model fails to accurately match various channel conditions. In contrast, the transformer-based method is able to achieve substantial performance gain over model-based methods by effectively extracting temporal-frequency-spatial correlations, which are critical in CSI completion. Nevertheless, a considerable performance gap remains between the transformer-based method and the case with perfect CSI. By integrating noise-plus-interference mechanism into channel estimation and completion, the proposed method is able to produce channel representations that well reflect the true channels, thereby outperforming all other solutions in the downstream task.

Fig. 7 and Fig. 8 illustrate the NMSE trends of various methods with respect to the numbers of predicted sub-carriers ( $N_p$ ) and the number of downstream training samples ( $R_t$ ), respectively, where the SINR is 8dB. As is shown in Fig. 7 and Fig. 8, the proposed method consistently achieves the lowest channel prediction NMSE across all the considered settings of  $N_p$  and  $R_t$ , demonstrating its adaptability. Notably, we can observe from Fig. 8 that the proposed method with  $R_t = 25\%$  is able to outperform all the other solutions with  $R_t = 80\%$ . This is because that the channel representations produced by the proposed method contains richer and more discriminative channel characteristics, which facilitates easier and more data-efficient downstream training thereby mitigating the over-

fitting risk with limited labeled samples. Furthermore, the proposed method exhibits greater performance gains under favorable conditions, such as when fewer sub-carriers to be predicted (e.g.,  $N_p = 4$ ) or when more samples are available for downstream training (e.g.,  $R_t = 80\%$ ). These results highlight the strong potential of the proposed method for high-precision communication scenarios in future 6G systems, such as ultra-reliable low-latency communication (URLLC) and massive MIMO transmission, where accurate channel knowledge is of vital importance.

#### IV. CONCLUDING REMARKS

In this paper, we proposed a wireless channel foundation model with embedded noise-plus-interference suppression structure, which is able to extract accurate and universal channel representations with limited pilot overhead under imperfect environment with noise and interference. Simulation results demonstrate its superiority in empowering downstream tasks across diverse simulation settings, highlighting its strong potentials for enhancing transmission performance and sensing accuracy, as well as overcoming the scarcity of labeled data, in future 6G systems.

#### REFERENCES

- [1] X. Ma, Z. Gao, F. Gao, and M. D. Renzo, "Model-driven deep learning based channel estimation and feedback for millimeter-wave massive hybrid MIMO systems," *IEEE J. Select. Areas Commun.*, vol. 39, no. 8, pp. 2388-2406, Aug. 2021.
- [2] B. Zhou, X. Yang, S. Ma, F. Gao, and G. Yang, "Pay less but get more: A dual-attention-based channel estimation network for massive MIMO systems with low-density pilots," *IEEE Trans. Wireless Commun.*, vol. 23, no. 6, pp. 6061-6076, Jun. 2024.
- [3] S. Zhang, S. Zhang, Y. Mao, L. Yeung, B. Clerckx, and T. Q. S. Quek, "Transformer-based channel prediction for rate-splitting multiple access-enhanced vehicle-to-everything communication," *IEEE Trans. Wireless Commun.*, vol. 23, no. 10, pp. 12717-12730, Oct. 2024.
- [4] Y. Sheng, K. Huang, L. Liang, P. Liu, S. Jin, and Y. Li, "Beam prediction based on large language models," *arXiv preprint arXiv:2408.08707*, Feb. 2025.
- [5] Y. Zhu, L. Yu, L. Shi, J. Zhang, and G. Liu, "Multi-modal large models based beam prediction: An example empowered by DeepSeek," *arXiv preprint arXiv:2506.0592*, Jun. 2025.
- [6] T. Yang, P. Zhang, M. Zheng, Y. Shi, L. Jing, and J. Huang, "WirelessGPT: A generative pre-trained multi-task learning framework for wireless communication," *IEEE Net.*, early access, Jun. 2025.
- [7] B. Liu, S. Gao, X. Liu, X. Cheng, and L. Yang, "WiFo: Wireless foundation model for channel prediction," *Sci. China Inf. Sci.*, vol. 68, no. 6, Jun. 2025.
- [8] S. Alikhani, G. Charan, and A. Alkhateeb, "Large wireless model (LWM): A foundation model for wireless channels," *arXiv preprint arXiv:2411.08872*, Apr. 2025.
- [9] A. Alkhateeb, "DeeepMIMO: A generic deep learning dataset for millimeter wave and massive MIMO applications," in *Proc. IEEE Inf. Theory Appl. Workshop (ITA)*, San Diego, CA, USA, Feb. 2019, pp. 1-8.
- [10] K. He, X. Zhang, S. Ren, and J. Sun, "Deep residual learning for image recognition," *Proc. IEEE Conf. Comput. Vis. Pattern Recognit. (CVPR)*, Las Vegas, NV, USA, 2016, pp. 770-778.